ELSEVIER

Catalysis Today 56 (2000) 283–295

CATALYSIS TODAY

www.elsevier.com/locate/cattod

Prospects and problems of dense oxygen permeable membranes

Peter Vang Hendriksen [a,*], Peter Halvor Larsen [a], Mogens Mogensen [a], Finn Willy Poulsen [a], Kjell Wiik [b]

[a] *Materials Research Department, Risø National Laboratory, DK-4000 Roskilde, Denmark*

[b] *Department of Inorganic Chemistry, Norwegian University of Science and Technology, N-7034 Trondheim, Norway*

Abstract

The prospects of using mixed ionic/electronic conducting ceramics for syngas production in a catalytic membrane reactor are analysed. Problems relating to limited thermodynamic stability and poor dimensional stability of candidate materials are addressed. The consequences for these problems, of flux improving measures like minimization of membrane thickness and minimization of the losses due to oxygen exchange over the membrane surfaces, are discussed. The analysis is conducted on two candidate materials: $La_{0.6}Sr_{0.4}Co_{0.2}Fe_{0.8}O_{3-\delta}$ and $SrFeCo_{0.5}O_x$. Finally, experimental investigations of the dimensional stability of the latter material under reducing conditions are reported.

Keywords: Permeable membrane; Synthesis gas; Conducting ceramics; Oxygen permeable membranes; Synthesis gas; Mixed conducting ceramics

1. Introduction

Synthesis gas (syngas) is a mixture of CO and H_2. It is an important intermediate in the production of hydrogen and in conversion of methane to a range of value added products including paraffins, olefins and alcohols [1]. Important examples are hydrogen production for ammonia synthesis [2] and methanol synthesis [3]. The annual world production of ammonia and methanol is in the order of 10^8 and 10^7 tons, respectively [2,3].

Traditionally synthesis gas is produced by steam reforming of methane [4]

$$CH_4 + H_2O \leftrightarrow CO + 3H_2, \quad \Delta H_{800^\circ C} = 225\,\text{kJ/mol} \tag{1}$$

An alternative route is the partial oxidation of methane

$$CH_4 + 1/2O_2 \leftrightarrow CO + 2H_2, \quad \Delta H_{800^\circ C} = -23\,\text{kJ/mol} \tag{2}$$

Whereas the steam reforming process is strongly endothermic the latter process is slightly exothermic. Combining the two processes one may achieve a thermally self-sustained process, the so-called autothermal reforming. Due to down stream requirements in many of the technologically important processes, for example, in hydrogen and methanol production, it is necessary to use pure oxygen, rather than air, in the autothermal reforming process. The scheme is considered very attractive if the cost of the oxygen supply can be reduced [5]. The investment cost in a cryogenic oxygen plant may constitute up to 45% of the total investment cost [5]. There is thus a great incentive to search for other ways of supplying the oxygen. An alternative route that seems very promising, is to use an oxygen permeable membrane for the separation, and to combine the catalytic conversion (reaction 2) and

* Corresponding author. Fax: +45-4677-5758.
E-mail address: peter.hendriksen@risoe.dk (P.V. Hendriksen).

0920-5861/00/$ – see front matter
PII: S0920-5861(99)00286-2

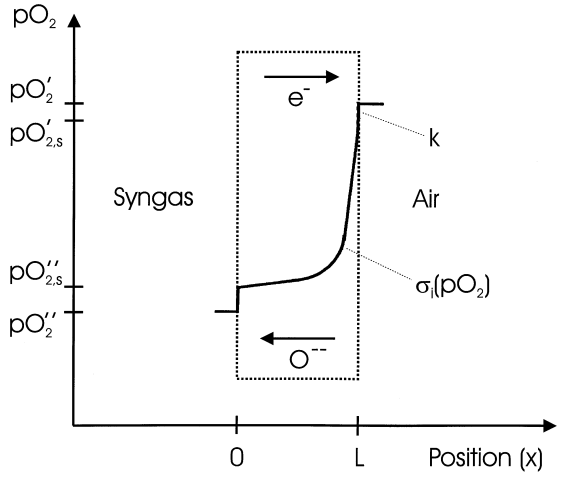

Fig. 1. Illustration of the principle in an MIEC syngas membrane. The solid curve illustrates a possible p_{O_2} profile over the membrane during operation. The profile is determined by the p_{O_2} dependence of the anion conductivity (σ_i) and the kinetics of the electrochemical processes at the surfaces (k). A single prime indicates air side, double prime syngas side, and subscript "s" that it is the equivalent p_{O_2} just inside the material.

the separation in a *catalytic membrane reactor*. This concept is currently being pursued by at least two international industrial consortia [6].

The membrane material to be used in such a reactor must meet a number of requirements. First of all it should be able to sustain a certain oxygen flux, the magnitude of which depends on the price of the membrane material, as well as the economics of the competing technology. Secondly, it must be sufficiently stable to allow long term operation at the relevant operating conditions, characterized by an operating temperature between 600 and 1000°C (the lower limit set by the temperature needed for the catalytic conversion and the upper by limitations of other plant components), and by exposure to both highly reducing environment (syngas side) and highly oxidizing environment (air side). Due to the requirement of high selectivity of oxygen to nitrogen, the focus in the membrane material development has been on oxide ion conductors, where the oxygen transport is mediated by oxide ions. For continuous operation a charge balancing electronic flux is needed. The principle is illustrated in Fig. 1. Depending on the mediator of the electronic flux the membranes may be divided in three different classes:

- A single material membrane, based on a material exhibiting both oxide ion conductivity and electronic conductivity (MIEC).
- A dual phase composite consisting of percolating phases of an ion conductor and an electron conductor.
- An oxide ion electrolyte, with suitable electrodes connected to an external circuit for the electronic current.

The scope of this paper is to analyse prospects and problems for the first of the above classes of membranes. Especially, two sets of problems will be discussed:

1. Problems relating to limited thermodynamic stability of the membrane materials.
2. Problems of mechanical integrity, arising due to the dimensional instability of the membrane material, when exposed to an oxygen activity gradient.

1.1. Oxygen permeation in solid MIEC membranes

The performance of a number of potential materials as oxygen permeation membranes for a syngas catalytic membrane reactor is summarised in Table 1. A recent comprehensive review of the field of dense oxygen permeable membranes can be found in Ref. [7]. The three first materials in Table 1 belong to the same class of materials. They are acceptor doped perovskites. In a general form, this class of materials may be written

$$Ln_{1-x}Ae_xTm1_yTm2_{1-y}O_{3-\delta} \quad (3)$$

Table 1
Reported oxygen fluxes through candidate materials for a syngas membrane reactor under conditions —first line is the membrane thickness, second line the temperature and third line the gases used in the experiment

Material	O_2 flux (ml cm^{-2} min^{-1})	Conditions	Ref.
$SrCo_{0.8}Fe_{0.2}O_{3-\delta}$	3	1 mm 875°C He/air	[8]
$La_{0.2}Ba_{0.8}Fe_{0.8}Co_{0.2}O_{3-\delta}$	4	0.55 mm 850°C, 1000 h syngas/air	[34]
$La_{0.2}Sr_{0.8}Co_{0.8}Fe_{0.2}O_{3-\delta}$	0.8	2–3 mm 900°C, 350 h syngas/air	[32]
$SrFeCo_{0.5}O_x$	3	0.25–1.2 mm 900°C syngas/air	[39]

The A-site ion is a lanthanide, Ln = La (Pr, Nd, Sm, Gd) or an alkaline earth, Ae = Ca, Sr, Ba, and the B-site is occupied by one or two different transition metals, Tm1 = Cr, Mn, Fe, Co and Tm2 = Co, Ni, Cu. Since the early studies by Teraoka et al. [8], a wide range of materials belonging to this class of materials has been investigated as oxygen separation membranes (see Ref. [7] for a review). Their use stems from the fact that they may exhibit high degrees of oxygen deficiency and that the mobility of the oxide ion vacancies may be relatively high ($D_v \approx 10^{-5}$–$10^{-6}\,cm^2\,s^{-1}$ at 1000°C). The high electronic conductivity is due to the capability of the transition metals to exist in different valence states in the structure.

The last material in Table 1, $SrFeCo_{0.5}O_x$, was suggested for this use by Balachandran et al. [9]. The material belongs to the more general class $Sr_4Fe_{6-x}Co_xO_{13+\delta}$. For $x \leq 1.5$, these materials are single phase [10]. They are isostructural with $Sr_4Fe_6O_{13}$, which has an orthorhombic intergrowth structure, where perovskite layers alter with $Fe_2O_{2.5}$ layers [7,10–12]. For $x \geq 1.5$, the material is a multi-phase material consisting of the intergrowth phase, a perovskite phase, $Sr(Fe, Co)O_3$, and CoO impurities [10–12]. From the observation that the oxide ion conductivity increases with increasing p_{O_2}, it has been suggested that the oxygen permeation in these materials occurs via interstitial oxygen [13].

In addition to the pure perovskites and the intergrowth structures described above, a third-class of perovskite related materials, namely brownmillerites, has been investigated as oxygen permeation membranes [14–16]. Performances under syngas relevant test conditions comparable to the performances given in Table 1 have been reported [17] for brownmillerite type materials.

Bredesen and Sogge [5] have performed an economic analysis, where they compare the catalytic membrane reactor route for syngas production with traditional autothermal reforming. They report, that if a membrane material cost of $1600\,\$/m^2$ can be met, the membrane should support an oxygen flux of ca. $10\,ml\,cm^{-2}\,min^{-1}$ (corresponding to a current density of $2.7\,A/cm^2$) to compete with the traditional route. Given the constituents of the materials in Table 1, the material cost target does not seem out of reach. The reported experimental fluxes, summarized in Table 1, fall short of the requirement by a factor of 2–10, however, there seems to be a number of straightforward possibilities for improving membrane performance.

The driving force for the transport of oxygen through the membrane is the difference in oxygen activity between the syngas side and the air side. The driving force is lost, partially over the membrane, due to limited anion conductivity, and partially at the two surfaces due to non-ideality of the electrochemical processes. This is illustrated schematically in Fig. 1. If the losses over the membrane are dominating, one may improve performance by reducing the membrane thickness. From SOFC research it is well known that gas-tight electrolytes with thickness down to ca. $40\mu m$ can be prepared on thick supports [18]. If the kinetics of the electrochemical processes (the exchange of oxygen over the surfaces of the membrane) is limiting, it is likely that performance may be improved by optimisation of the surfaces, e.g. by enhancing the surface area and/or addition of suitable catalytic materials. Considering that the results quoted in Table 1 were for self-standing unoptimized membranes the prospects for the technology look good, as judged from considering only requirements of membrane cost and transport properties. However, a number of problems may be encountered when introducing the above presented flux-improving changes. Improving the electrode performance may, as shall be shown, have a negative effect on the stability of the membrane. Reducing the membrane thickness to the level where a support is needed raises a number of mechanical issues. In the following sections we shall discuss the effects on thermodynamic and mechanical stability of introduction of the suggested changes.

2. Theory

2.1. Calculation of permeation flux and p_{O_2} profile

The oxygen flux through a mixed conducting membrane of thickness L, subjected to different oxygen activities at the two sides, can be calculated from the Wagner equation [19,20]

$$J_{O_2} = \frac{RT}{16F^2L}\int_{\ln p''_{O_2,s}}^{\ln p'_{O_2,s}} \frac{\sigma_e\sigma_i}{\sigma_e+\sigma_i}\,d\ln p_{O_2} \quad (4)$$

where F is Faraday's constant, R the gas constant, T the temperature and σ_e and σ_i signifies electronic and ionic conductivity, respectively. $p'_{O_{2,s}}$ and $p''_{O_{2,s}}$ are the equivalent oxygen partial pressures in the outermost layers of the membrane on the air side and the syngas side of the membrane, respectively (cf. Fig. 1). Eq. (4) may be evaluated numerically from experimental data on the p_{O_2}-dependences of the ionic and electronic conductivities. In some cases the behaviour of the materials is well described by simple point defect models and it may be possible to integrate Eq. (4) analytically. van Hassel et al. [21] have presented an analytical solution to Eq. (4) applicable for a number of acceptor doped perovskite materials.

In addition to the loss over the bulk of the membrane ($p'_{O_{2,s}} - p''_{O_{2,s}}$) there is a loss of driving force associated with non-ideality of the electrochemical reactions. At the air side of the membrane (the cathode) molecular oxygen is dissociated, reduced and incorporated in the membrane as oxide ions

$$\tfrac{1}{2}O_2 + 2e^- \rightarrow O^{2-} \tag{5}$$

At the syngas side of the membrane (the anode), oxide ions are released from the lattice. The overall anode process may be written

$$CH_4 + O^{2-} \rightarrow CO + 2H_2 + 2e^- \tag{6}$$

Here, we shall not try to analyse the reaction pathways and possible elementary steps of the electrode reactions, but simply assume that the overall electrode processes follow linear electrode kinetics, i.e., that the electrode overpotentials are simply proportional to the current density, I_{O_2}:

$$\eta_{an} = I_{O_2} r_{an} = -\frac{RT}{4F} \ln\left\{\frac{p''_{O_2}}{p''_{O_{2,s}}}\right\} \tag{7}$$

$$\eta_{cat} = I_{O_2} r_{cat} = -\frac{RT}{4F} \ln\left\{\frac{p'_{O_2}}{p'_{O_{2,s}}}\right\} \tag{8}$$

Here subscripts "an" and "cat" indicate anode and cathode, respectively, and r is the effective area specific polarization resistance. Only little experimental material is available on the performance of the electrodes on MIEC syngas membranes. Linear kinetics were chosen because of simplicity and lack of specific knowledge about the kinetics for the relevant materials under relevant conditions. However, it should be noted that SOFC electrodes are often found to exhibit linear kinetics even under strong polarization [22]. The rate of the cathode process may be estimated from O^{16}/O^{18} isotope exchange experiments [23], and the rate of the anode process may be estimated from conductivity relaxation experiments [24]. The surface exchange rate constant, k, obtained from an isotope exchange experiment is related to the area specific polarization resistance by

$$r_{cat} = \frac{RT}{16F^2 C_O} \frac{1}{k} \tag{9}$$

where C_O is the oxide ion concentration in the perovskite. In steady state, the flux across the surfaces must equal the flux in the bulk, i.e.

$$J_{O_2} = I_{O_2}/4F \tag{10}$$

By solving Eqs. (4),(7),(8) and (10), one may calculate the permeation flux through the membrane, taking into account both losses in the bulk and at the electrodes. Numerical solution of the problem is straightforward. We adopted a simple iterative method. From a start guess of $p'_{O_{2,s}}$ and $p''_{O_{2,s}}$, an estimate of the flux was calculated from Eq. (4). This flux was used to estimate the electrode losses by Eqs. (7) and (8). From the initial guess and the calculated electrode losses a better estimate of $p'_{O_{2,s}}$ and $pO''_{2,s}$ was constructed and so forth until convergence.

The p_{O_2} profile through the bulk of the membrane may also be constructed from Eq. (4). In steady state, the flux through any slab of the material must be the same, i.e. one may find the p_{O_2} at position x by requiring that the integral evaluated between 0 and x, with integration limits $p''_{O_{2,s}}$ and $p_{O_{2,x}}$, equals the integral evaluated between 0 and L with integration limits $p''_{O_{2,s}}$ and $p'_{O_{2,s}}$.

2.2. Calculation of mechanical stresses

For the acceptor doped perovskite materials it is well known that the unit cell volume changes with changes of stoichiometry [25,26] and thereby with changes of p_{O_2}. In general the membrane is not free to deform according to any p_{O_2}-profile, and therefore the volume expansion will lead to a build-up of mechanical stresses. This problem was analyzed for the case of thin plates (used as interconnects in SOFC stacks) in

Refs. [27–29]. Here we shall consider a tubular membrane, self-standing or supported on a porous support. The membrane thickness is assumed to be much smaller than the diameter of the tube, and the p_{O_2} is assumed to vary only in the radial (x) direction. The biaxial stress field, $\sigma(x) = \sigma^{\phi}(x) = \sigma^{z}(x)$, developing in a tubular membrane due to the lattice expansion induced strain, ϵ_{le}, is given by Hooke's law

$$\sigma_j(x) = \frac{E_j}{1-\nu_j}(\epsilon - \epsilon_{j,le}(x)) \tag{11}$$

where

$$\epsilon_{j,le}(x) = \begin{cases} \epsilon_{le}(x), & j = 1, \text{ membrane} \\ 0, & j = 2, \text{ support} \end{cases} \tag{12}$$

where j is a layer index, E the Young's modulus and ν is the Poisson's ratio. ϵ is the overall biaxial strain, i.e. the actual expansion of a volume-element, when it is not allowed to expand freely to adjust to the local p_{O_2}, but is constrained as a part of an elastic body. It is assumed here that there is no lattice expansion in the support. For a tubular membrane the overall strain, ϵ, will because of the rotational symmetry be independent of x. The lattice expansion due to the p_{O_2}-profile thus results in a mere expansion in axial and circumferential directions, given by

$$\epsilon = \frac{E_m/(1-\nu_m)}{E_s L_s/(1-\nu_s) + E_m L/(1-\nu_m)} \int_0^L \epsilon_{le}(x)\,dx \tag{13}$$

where m indicates membrane, and s indicates support. Eq. (13) follows directly from the requirement of overall force–equilibrium.

In the following section, we shall use Eqs. (11)–(13) to calculate the maximum tensile stresses in free, as well as supported membranes under various changes in membrane design, and under various assumptions on electrode kinetics. Evidently (cf. Eq. (11)), one must know the lattice expansion induced strain profile in the material. This is derived combining experimental data on expansion as a function of p_{O_2} with the calculated p_{O_2}-profiles (see previous section).

2.3. Fracture mechanical considerations

In fracture mechanics one compares the energy release rate, G, under a certain mode of failure (a calculated value) with a critical value, G_c, which is a characteristic of the material, that expresses the energy needed per unit area to create a new surface. If, for a given crack propagation mode; $G < G_c$, an initial crack will not grow. Considering a thin dense membrane on a porous support of the same material. (Choosing the support material to be the same as the membrane material one circumvents problems of undesired reactions between membrane and support and problems arising from TEC-mismatches.) When used as a syngas membrane reactor the whole support is subjected to the same p_{O_2} (neglecting mass-transfer limitations inside the support), whereas the membrane is subjected to a p_{O_2} gradient. Hence, the membrane layer and the support will in general expand (or contract) to different degrees resulting in a build up of mechanical stresses and a storage of elastic energy in the reactor. If the two layers delaminate this energy will be released. We shall consider a design criterion ($G_{ss} < G_c$) based on the steady state energy release rate of delamination. The advantage of this approach is that one does not have to consider the complex stress/strain fields around the crack tip [30,31]. Under steady state crack propagation the situation around the tip of the crack does not change, the net result of a certain propagation of the crack is conversion of a slab of the tube from intact (far ahead of the crack) to delaminated (in the wake of the crack) [30]. Hence, the energy released per unit area as the crack propagates is simply the difference in stored energy per unit area between an intact tube and a delaminated one

$$\begin{aligned} G_{ss} &= U_{\text{intact}} - U_{\text{delaminated}} \\ &= \int_0^{L_{tot}} \sigma(x)(\epsilon - \epsilon_{le}(x))\,dx \end{aligned} \tag{14}$$

where $\sigma(x)$ is given by Eq. (11) and ϵ_{le} is given by Eq. (12) (i.e. a system where the support does not expand is considered). In the second equation it was assumed that after a complete delamination between support and membrane, the system is free of elastic energy. The design criterion above is relevant for the case where initial flaws are very large (as judged on the length scale of the supported membrane). If initial flaws are small on this length scale the criterion is very conservative. A local delamination around an initial small flaw is much less effective for releasing the stored elastic energy than the steady state delamina-

tion considered. One may also be sceptic as to whether steady state crack propagation will ever be reached in the present system. Before steady state is reached the membrane will break because it has lost its support leading to a "catastrophic" series of events due to direct mixing of gasses, however, we believe that the analysis, despite the above discussed weaknesses, may show important trends relevant for membrane reactor design.

3. Results and discussion

Two membrane materials are analysed: a $La_{0.6}Sr_{0.4}Co_{0.2}Fe_{0.8}O_{3-\delta}$ perovskite and the "Balachandran material": $SrFeCo_{0.5}O_x$. These materials were chosen because they are relatively well investigated, and most of the parameters needed for the analysis can be found in literature. For the first material we shall analyse both problems relating to thermodynamic and mechanical stability, whereas only mechanical issues are addressed for $SrFeCo_{0.5}O_x$.

3.1. Thermodynamic stability

To calculate the oxygen permeation flux and the p_{O_2} distribution over the syngas membrane, the polarization resistances characterising the electrochemical reactions must be known. Two different estimates were considered. From the surface exchange rate constant determined by Lane et al. [23] for $La_{0.6}Ca_{0.4}Co_{0.2}Fe_{0.8}O_{3-\delta}$, a value of $r_{cat} = r_{an} = 0.8\,\Omega\,cm^2$ was derived (cf. Eq. (9)). This value is taken to be a proven value for the electrode kinetics for the considered type of materials (in the following referred to as "slow" kinetics). It should be noted, however, that the surface exchange rate is not a pure material property. It depends on the surface morphology and therefore on sample preparation. Furthermore, the properties of these perovskites do in general depend on which alkaline earth element is chosen as a dopant [32,34]. A value 10 times smaller, $0.08\,\Omega\,cm^2$, was taken to be illustrative of what may be achievable after optimization of the electrodes (fast kinetics). At cathodes in solid oxide fuel cells such rates for the oxygen reduction process have been proven [35].

The losses in the bulk of the membrane were evaluated using the analytic solution to Eq. (4) derived by van Hassel et al. [21] for acceptor doped perovskites, where the oxide ion conductivity can be taken to be proportional to the oxide ion vacancy concentration ($\sigma_i \propto V_O^{\bullet\bullet} D_v$). The vacancy concentration is determined considering three defect reactions (for simplicity written for the pure ferrite)

$$SrFeO_3 \underset{LaFeO_3}{\rightarrow} Sr'_{La} + Fe^{\bullet}_{Fe} + 3O^{x}_{O} \quad \text{(aliovalent doping)} \tag{15}$$

$$2Fe^{\bullet}_{Fe} + O^{x}_{O} \leftrightarrow 2Fe^{x}_{Fe} + V^{\bullet\bullet}_{O} + \tfrac{1}{2}O_2(g) \quad \text{(redox process)} \tag{16}$$

$$2Fe^{x}_{Fe} \leftrightarrow Fe'_{Fe} + Fe^{\bullet}_{Fe} \quad \text{(charge disproportionation)} \tag{17}$$

The equilibrium constants of the two last reactions must be known to use van Hassel's treatment. They were estimated by fitting the predictions of the simple point defect model outlined above to experimental data [36] on the p_{O_2} dependence of the ionic conductivity of the material. Anderson [36] found that the ionic conductivity increased with decreasing p_{O_2} from ca. $0.01\,S\,cm^{-1}$ in air to a plateau value of ca. 0.3 S/cm between $p_{O_2} = 10^{-5}$atm and $p_{O_2} = 10^{-12}$ atm at 800°C. Whereas the considered point defect model represents very well the behaviour of (La, Sr)FeO_3 it is clear from the experimental investigations of this material by Tai et al. [37,38], that it does not give a fully adequate description of the changes occurring in $La_{0.6}Sr_{0.4}Co_{0.2}Fe_{0.8}O_{3-\delta}$ with changes of p_{O_2}, however, for the present purpose the model is adequate, as the parameters may be chosen so the model fits well the experimentally observed p_{O_2} dependence of the conductivity, which is the relevant property for evaluation of the permeation flux.

The thickness dependence of the oxygen flux through the perovskite membrane is illustrated in Fig. 2 for oxygen partial pressures of 0.2 atm and 1×10^{-19}atm at the air and syngas side of the membrane, respectively. Assuming a polarisation resistance of $0.8\,\Omega\,cm^2$ (slow kinetics), the flux through the membrane is limited by the surface exchange processes. There is hardly any improvement on reducing the thickness of the membrane by a factor of 10. The equivalent oxygen partial pressures just inside

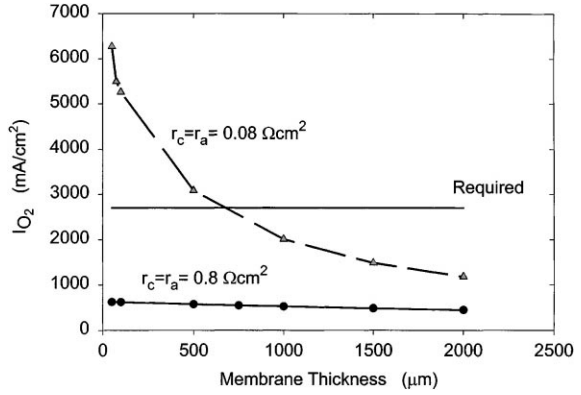

Fig. 2. Calculated oxygen fluxes as a function of membrane thickness for a $La_{0.6}Sr_{0.4}Co_{0.2}Fe_{0.8}O_{3-\delta}$ membrane under the assumption of "slow" (full curve) and "fast" (dashed curve) electrode kinetics. The p_{O_2} at the syngas side was 10^{-19} and 0.2 atm on the air side, and the temperature was 800°C (base case). The thin horizontal line indicates an estimate of the flux needed for the membrane route to be economically interesting.

the membrane at either side are plotted as a function of membrane thickness in Fig. 3. For slow kinetics most of the driving force is seen to be lost at the surfaces. If a polarization resistance 10 times smaller is assumed, the flux is seen to vary inversely proportional to the thickness of the membrane, as expected when the process is limited by diffusion in the bulk. If one can modify the surface on this material, as to

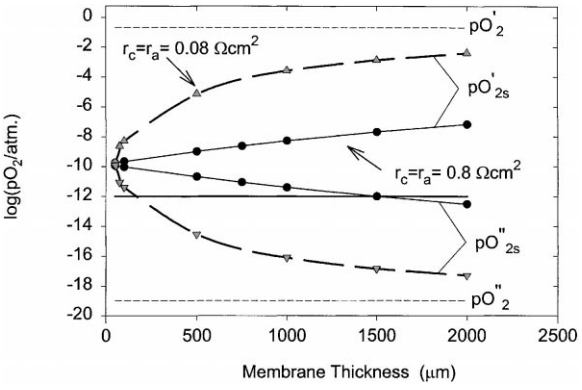

Fig. 3. Calculated oxygen partial pressures in the outermost layers at both sides ($p''_{O_{2,s}}$ ~ syngas) and ($p'_{O_{2,s}}$ ~ air side) of a $La_{0.6}Sr_{0.4}Co_{0.2}Fe_{0.8}O_{3-\delta}$ membrane plotted as a function of membrane thickness for the same conditions as in Fig. 2. The dashed curve corresponds to fast kinetics and the full curve to slow kinetics. The full horizontal line indicates the stability limit of the material, and the dashed horizontal lines p'_{O_2} and p''_{O_2}.

achieve a performance like known from solid oxide fuel cells, the flux through a syngas membrane of this type will exceed the flux requirement derived from the economic analysis (horizontal line in Fig. 2).

The gas at the syngas side of the membrane defines a p_{O_2} much lower ($\approx 10^{-19}$atm) than the stability limit of the present material (illustrated by the thin horizontal line in Fig. 3), however, due to flux of oxygen through the membrane, the p_{O_2} is higher in the outermost layer of the membrane than in the gas phase (syngas side). Depending on membrane thickness and electrode kinetics all the membrane may experience a p_{O_2} above the stability limit. For slow kinetics this is the case as long as the membrane is thinner than 1.5 mm, and for fast kinetics as long as the membrane is thinner than ca. 100 μm (cf. Fig. 3). Evidently, the faster the cathode process is in comparison to the anode process the easier it will be to stay above the stability limit. It may be easily shown that membrane operation entirely inside the stability window of the material ($p_{O_2} > p_{O_{2,stab}}$) is not possible unless the cathode kinetics fulfill the requirement

$$r_{cat} \leq r_{an} \frac{\log\{p'_{O_2}/p_{O_{2,stab}}\}}{\log\{p_{O_{2,stab}}/p''_{O_2}\}} \tag{18}$$

Inserting values for the considered perovskite the requirement to the cathode is that the polarisation resistance must be less than 1.6 times the anode polarisation resistance. Note, that this is a necessary but not sufficient requirement, i.e. equality in Eq. (18) corresponds to letting the membrane thickness approach 0.

It is interesting to note, that though the above requirement is not initially fulfilled it may become fulfilled as the material decomposes. A decomposed zone starting from the syngas side of the membrane will only extend inwards in the membrane to the $p_{O_{2,stab}}$-isobar. If the decomposed material has poorer ionic conductivity than the starting material, if the decomposition of the surfaces reduces the reaction rates of the electrochemical processes, and if the decomposed layer is not porous, then it is likely that only a thin decomposed layer will form on the syngas side of the membrane, i.e. the material is self-protecting. The possibility of such a behaviour was also pointed out by Bouwmeester and Burggraaf [7], and in a study of $La_{0.2}Ba_{0.8}Fe_{0.8}Co_{0.2}O_3$, Tsai et al. [34] reports observations that could indicate such a mechanism.

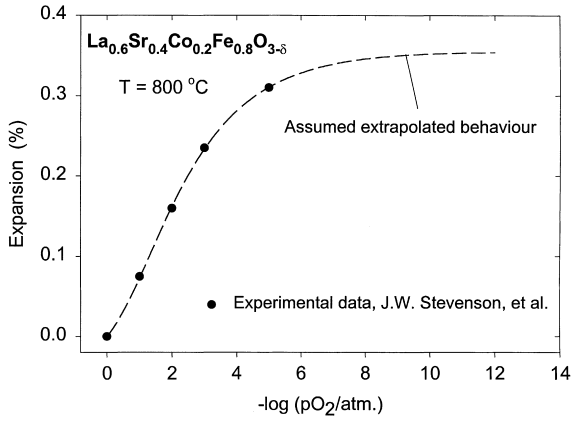

Fig. 4. Estimated isothermal expansion on reduction for $La_{0.6}Sr_{0.4}Co_{0.2}Fe_{0.8}O_{3-\delta}$ at 800°C. The symbols are the experimental data obtained by Stevenson et al. [32] and the dashed curve is the assumed extrapolated behaviour (see text).

3.2. Mechanical problems

3.2.1. Perovskite material

The dimensional stability of $La_{0.6}Sr_{0.4}Co_{0.2}Fe_{0.8}O_{3-\delta}$ was investigated by Stevenson et al. [32] by isothermal dilatometry in the p_{O_2} range from 1 atm to 1×10^{-5} atm. To asses the mechanical consequences of the dimensional instability in a syngas reactor it is necessary to estimate the material behaviour in a wider p_{O_2}-range. In Fig. 4 the assumed material behaviour is plotted together with the experimental results of Stevenson et al. [32]. The extrapolated curve was constructed by curve-fitting to the experimental data under the requirement that the expansion should level off with reducing p_{O_2}. The reason for the latter requirement, (which cannot be justified looking at the experimental data only) is that this is expected considering the underlying reason for the expansion. The expansion is caused by the gradual reduction of tetravalent cations to larger trivalent (and even divalent) transition metal ions as the p_{O_2} decreases. If one plots the average cation size, as calculated from the simple point defect model discussed previously, one finds a curve similar to the fitting curve in Fig. 4. For the chromites, where experimental investigations are available in much larger p_{O_2} ranges, such shapes of the p_{O_2} dependence of the expansion are found.

The calculated p_{O_2} profile inside the membrane under base case conditions (a p_{O_2} of 10^{-19}atm at the syngas side and 0.2 atm on the air side and a temperature of 800°C) is illustrated in Fig. 5. The values used for the other important parameters are given in the figure caption. (Note, that for the depicted case r_{cat} is half that of r_{an}.) The local lattice expansion induced strain (combining the calculated p_{O_2} profile and the assumed expansion curve) as well as the overall strain (ϵ) are also shown. The lattice expansion due to the p_{O_2}-gradient is seen to result in an overall expansion

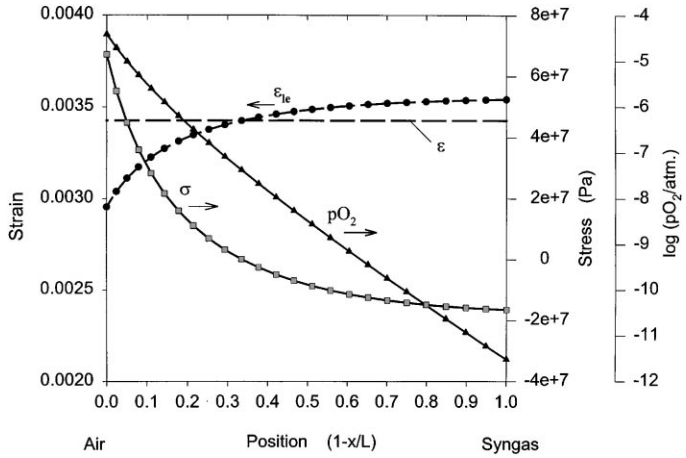

Fig. 5. Calculated $p_{O_{2-}}$, strain- and stress-profiles across a $La_{0.6}Sr_{0.4}Co_{0.2}Fe_{0.8}O_{3-\delta}$ membrane exposed to a p_{O_2} of 10^{-19} atm at the syngas side and a p_{O_2} of 0.2 atm on the air side ($T = 800$°C). The following values of the parameters were assumed: $r_{an} = 0.8\,\Omega\,cm^2$, $r_{cat} = 0.4\,\Omega\,cm^2$, $E = 100$ GPa and $\nu = 0.30$.

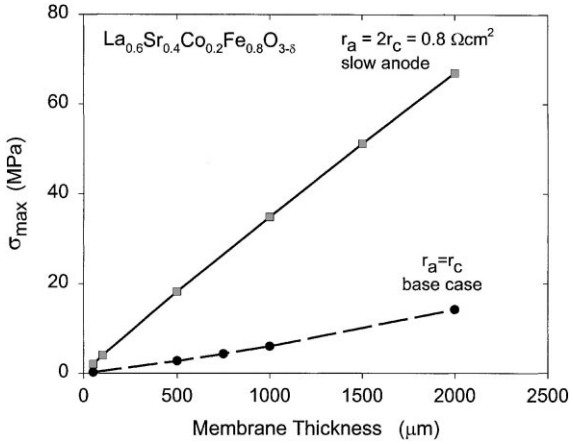

Fig. 6. Calculated maximum tensile stress in a syngas membrane of $La_{0.6}Sr_{0.4}Co_{0.2}Fe_{0.8}O_{3-\delta}$ under "base case" conditions (see caption of Fig. 2) as a function of membrane thickness under two different assumptions of the electrode kinetics.

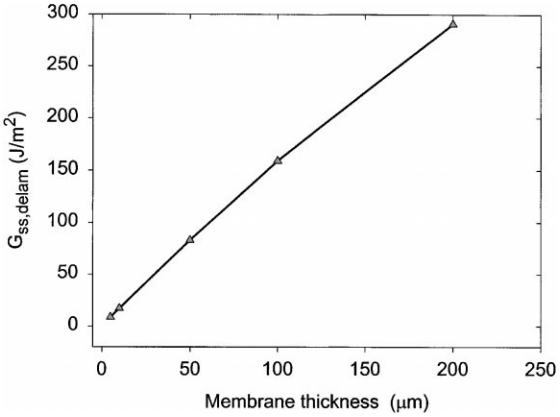

Fig. 7. Calculated elastic strain energy release rate as a function of membrane thickness for the case of a supported $La_{0.6}Sr_{0.4}Co_{0.2}Fe_{0.8}O_{3-\delta}$ membrane under "base case" conditions. The membrane thickness was 50μm. The thickness of the support was 2 mm and an *E*-modulus of 50 GPa was assumed.

of the membrane of ca. 0.35%. Tensile stresses build up at the air side and compressive stresses at the syngas side.

In Fig. 6, the maximum tensile stress occurring in the membrane under base case conditions is plotted as a function of membrane thickness. The stress level increases with increasing membrane thickness, reflecting that the thicker the membrane is, the larger is the p_{O_2} difference over it, and consequently, the larger will be the difference in local lattice expansion and mechanical stresses. Calculations were performed also for different electrode polarization resistances at the two sides. If the cathode kinetics are faster than the anode kinetics the maximum tensile stresses are much higher than for the case of equal polarization resistances (cf. Fig. 6). The maximum tensile stress is located close to the air side surface. It is proportional to the difference between overall expansion and local lattice expansion. When improving the cathode performance relative to the base case, the $p'_{O_{2,s}}$ increases, and the local lattice expansion decreases correspondingly, resulting in a larger tensile stress. Even faster kinetics will lead to a further increase of the stress levels. For membrane thickness from 0.5 to 1 mm the tensile stress levels reached with the assumed values of the electrode kinetics and anion conductivity are not likely to be detrimental (for an optimized ceramic). Hence, whether the dimensional instability depicted in Fig. 4 is tolerable or not becomes a question of both mechanical properties and electrode performances. Mechanical failures caused by insufficient dimensional stability of ceramics exposed to a p_{O_2}-gradient have been reported both for potential syngas membrane materials [33] and for SOFC interconnect materials [29].

If the membrane is thinner than a few hundred μm it must be supported on a porous substrate. If the substrate is on the air side of the membrane it will experience no expansion. When operating as a reactor the membrane will therefore be in compression and the substrate in mild tension. For this case the relevant failure mode is not breakage of the membrane due to the levels of tensile stresses but rather a delamination between membrane and support. Calculated energy release rates for a delamination are plotted in Fig. 7 as a function of the thickness of the membrane. The conditions were the base case conditions and a support thickness of 2 mm was assumed. In Fig. 8 the calculated energy release rate is plotted as a function of overall expansion of the membrane for a fixed membrane thickness (again considering base case conditions). The elastic constants assumed are given in the figure captions. Here the term overall expansion means the expansion (ϵ) that a free membrane would experience when exposed to the same p_{O_2} gradient. *G* is seen to scale with the overall expansion squared and

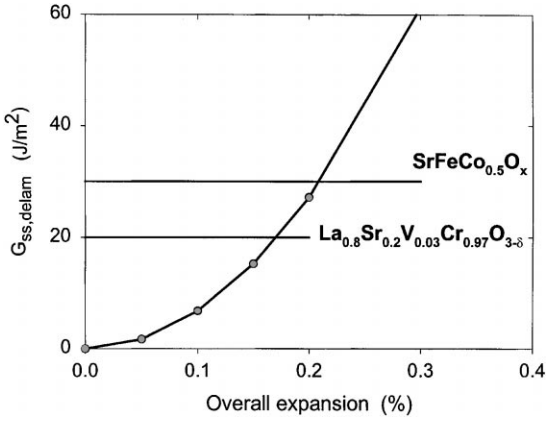

Fig. 8. Calculated elastic strain energy release rate for delamination in a $La_{0.6}Sr_{0.4}Co_{0.2}Fe_{0.8}O_{3-\delta}$ membrane reactor with a supported membrane as a function of the overall expansion of the membrane. The term "overall expansion" refers to the expansion that a free membrane would experience when exposed to the considered p_{O_2}-gradient. The membrane thickness was 50 μm. The thickness of the support was 2 mm and an *E*-modulus of 50 GPa was assumed. Critical energy release rates derived from measured fracture toughnesses of two relevant ceramics are indicated by horizontal lines for comparison.

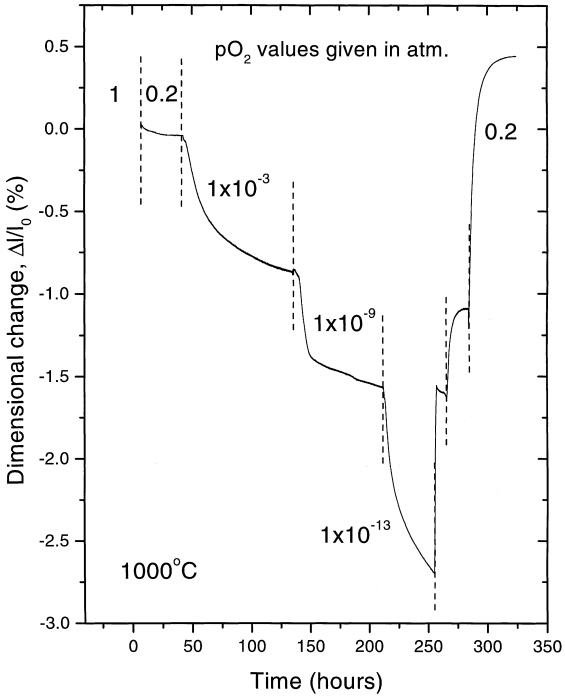

Fig. 9. Measured dimensional change of a bar of $SrFeCo_{0.5}O_x$ when exposed to various oxygen partial pressures at 1000°C.

with the membrane thickness in a linear way. Clear suggestions for minimizing the risk of failure follow directly from the two plots.

The high temperature fracture toughness of the considered perovskite is not known to us. G_c-values for two other membrane relevant ceramics are plotted in Fig. 8 for comparison. Assuming that the toughness of the investigated material is similar to these materials fulfilment of the suggested design criterion is seen to require an overall expansion under the specified experimental conditions of less than 0.2%.

Only loads introduced by the p_{O_2}-gradient across the membrane were considered in the present analysis. This was chosen for simplicity, and from an a priori expectation that this load case is the most critical one. There is a number of other load cases, that should be taken into account when optimizing the membrane design according to mechanical considerations. The gas composition will change down-stream as methane is consumed, and so will the temperature under operation. Hence, both thermal strains and lattice expansion induced strains will vary along the axis of the tube, resulting in build up of stresses. Also the situation at room temperature should be considered. If the thermal expansion coefficient of the membrane material differs from that of the support, stresses will build up during cooling. Finally, effects of possible (and likely) pressure differences across the membrane must be taken into account in the mechanical analysis.

3.2.2. $SrFeCo_{0.5}O_x$

To our knowledge, no investigations of the dimensional stability of $SrFeCo_{0.5}O_x$ over the full p_{O_2} interval relevant for a syngas membrane have been reported in the literature, and therefore an experimental investigation by dilatometry was undertaken in the present study. Samples were prepared by the mixed oxide route and bars for the dilatometer were pressed and sintered at 1200°C. The dimensions of the investigated bars were $18 \times 3 \times 6.5\,mm^3$. The experimental data are depicted in Fig. 9. A strong contraction is observed when exposing this material even to mildly reducing conditions. When switching back to air after the reduction sequence the sample is seen to have suffered a net expansion.

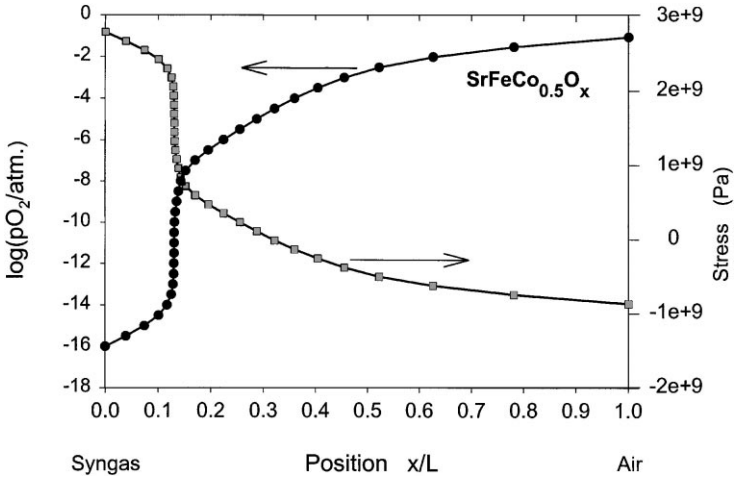

Fig. 10. Calculated p_{O_2}-profile and stress-profile over a $SrFeCo_{0.5}O_x$ membrane exposed to air and a p_{O_2} of 10^{-16} atm at either side at 1000°C. Reversible electrode kinetics were assumed. $E = 124$ GPa and $\nu = 0.30$.

Several investigators [10–12] have reported that at room temperature the materials with nominal composition $Sr_4Fe_{6-x}Co_xO_{13\pm\delta}$ consist of multiple phases for $x > 1.5$. For the composition investigated here with $x = 2$ the material consists of three phases: a phase isostructural with $Sr_4Fe_6O_{13}$, a $SrFe_{1-y}Co_yO_{3-\delta}$ perovskite/brownmillerite and CoO [10–12]. A powder sample was investigated by high temperature X-ray diffraction at the same oxygen activities that were used in the dilatometry experiment. The X-ray investigations confirmed the multi-phase character of the sample and showed that reducing the p_{O_2} lead to an increase in the amount of (Co, Fe)O and perovskite at the expense of the layered phase. At the lowest p_{O_2}, metallic Co was detected. These species all have higher density than the layered structure, and the contraction observed upon reduction in the dilatometer, thus seems to be caused by the p_{O_2} driven phase changes.

Like for the perovskites the mechanical consequences of the dimensional instability depicted in Fig. 9 were analysed. The p_{O_2} profile across a membrane was calculated by numerical integration of Eq. (4) using the conductivity data reported by Ma et al. [13]. Reversible kinetics were assumed at both surfaces, and a p_{O_2} of 10^{-16} atm on the syngas side and 0.2 atm at the air side was assumed. The following values were used for the mechanical constants $E = 124$ GPa and $\nu = 0.3$ [39]. The calculated p_{O_2} profile as well as the stresses introduced by the dimensional instability are depicted in Fig 10. The syngas side of the membrane is in tension and the air side in compression. The maximum tensile stress was found to be 300 MPa!, which is far higher than the fracture strength of the material. Yet, this material has been demonstrated capable of functioning as a syngas reactor for hundreds of hours [39], so some of the assumptions made leading to the predictions of such high stresses must be erroneous. We believe that it is probably the assumption of reversible kinetics at the syngas side (resulting in $p''_{O_{2,s}} = p''_{O_2}$) that is wrong, and that the material is effectively "protected" by slow kinetics or possibly a decomposed layer (with poorer transport properties) at the syngas side.

4. Conclusion

The prospects of developing materials (MIECs) for membrane reactors for syngas production with sufficiently good transport properties as to render the technology economically competitive seem good. However, performance has to be improved relative to present day state-of-the-art. Improvement of the electrode performance by catalyst addition or enhancement of the surface area has to be introduced considering its effects for the stability of the membrane. Slow kinetics at the anode may protect the

material from the syngas environment, and improvement of the anode performance has to be matched by improvement of cathode performance (cf. Eq. (18)) (and possibly a reduction of membrane thickness) to assure membrane operation within the stability limits of the material. Reduction of membrane thickness to the level where a support is needed may be difficult for the perovskite materials due to their dimensional instability in reducing environment. A fracture mechanical analysis was presented providing a rational basis for formulating material requirements and optimization of reactor design. An expansion on reduction of 0.35%, as reported for $La_{0.6}Sr_{0.4}Co_{0.2}Fe_{0.8}O_{3-\delta}$ seems too high, and a delamination between membrane and support is likely.

$SrFeCo_{0.5}O_x$ was found to contract up to 2.5% on reduction. High temperature X-ray diffraction indicated that the contraction is caused by p_{O_2} driven phase changes in the sample. The fact, that membrane reactors in this material has operated for many hundreds of hours indicates that the material is protected towards the low p_{O_2} in the syngas by poor anode kinetics or by a thin decomposed layer with poorer transport properties.

Acknowledgements

J. Kjøller is acknowledged for his assistance with the dilatometry experiments.

References

[1] J.G.L. Fierro, Catal. Lett. 22 (1993) 67.
[2] B. Elvers, S. Hawkins, G. Shulz (Eds.), Ullmann's Encyclopaedia of Industrial Chemistry, vol. A16, 5th completely rev. ed., VCH, Wienheim, 1990, p. 482.
[3] W. Gerhartz, Y.S. Yamamoto, F. Thomas Cambell, R. Pfefferkorn, J.F. Rounsaville (Eds.), Ullmann's Encyclopedia of Industrial Chemistry, vol. A2, 5th completely rev. ed., VCH, Wienheim, 1985, p. 230.
[4] J.R. Rostrup-Nielsen, Catalytic Steam Reforming, Springer, Berlin, 1984.
[5] R. Bredesen, J. Sogge, Paper presented at: The United Nations Economic Commission for Europe Seminar on Ecological Applications of Innovative Membrane Technology in Chemical Industry, Chem/Sem. 21/R.12, 1–4 May 1996, Cetaro, Calabria, Italy.
[6] Press release from Praxair, July 1997; Press release from United States Department of Energy, May 1997.
[7] H.J.M. Bouwmeester, A.J. Burggraaf, in P.J. Gellings, H.J.M. Bouwmeester (Eds.), The CRC Handbook of Solid State Electrochemistry, CRC Press, Boca Ranton, 1997, p. 481 (Chapter 14).
[8] Y. Teraoka, H.M. Zhang, S. Furukawa, N. Yamazoe, Chem. Lett. (1985) 1743–1746.
[9] U. Balachandran, M.S. Kleefish, T.P. Kobylinski, S.L. Morissette, S. Pei, International Patent WO96/24065, 1994.
[10] S. Guggilla, A. Manthiram, , J. Electrochem. Soc. 144 (1979) L120.
[11] H. Fjellvåg, B.C. Hauback, R. Bredesen, J. Mater. Chem. 7 (1997) 2415.
[12] B. Ma, J.P. Hodges, J.D. Jorgensen, D.J. Miller, J.W. Richardson, U. Balachandran, J. Solid State Chem. 141 (1998) 576.
[13] B. Ma, U. Balachandran, J.H. Park, C.U. Segre, J. Electrochem. Soc. 143 (1996) 1736.
[14] M. Schwartz, J. White, A.F. Sammells, International Patent WO97/41060, 1996.
[15] J.B. Goodenough, A. Manthiram, A. Paranthanam, Y.S. Zhen, Solid State Ionics 52 (1992) 105.
[16] B.C.H. Steele, Mater. Sci. Eng. B 13 (1992) 79.
[17] A.F. Sammells, M. Schwartz, R.A. Mackay, T.F. Barton, D.R. Peterson, Catalysis Today 56 (2000) 327.
[18] S.C. Singhal, Proceedings of the Fifth International Symposium on SOFC, Aachen, 2–5 June 1997, The electrochemical Society, Proc. vol. 97-40, p. 37.
[19] C. Wagner, W. Schottky, Z. Phys. Chem. B 11 (1930) 25.
[20] L. Heyne, in: S. Geller (Ed.), Solid Electrolytes, Topics in Applied Physics, vol. 21, Springer, Berlin, 1977, p. 169 (Chapter 7).
[21] B.A. van Hassel, T. Kawada, N. Sakai, H. Yokokawa, M. Dokiya, Solid State Ionics 66 (1993) 295.
[22] M. Mogensen, S. Skaarup, Solid State Ionics 86–88 (1996) 1151.
[23] J.A. Lane, P.H. Middleton, H. Fox, B.C.H. Steele, J.A. Kilner, in: T.A. Ramanarayan, W.L. Worrel, H.L. Tuller (Eds.), Proceedings of the Second International Symposium on Ionic and Mixed Conducting Ceramics, The Electrochemical Society, Proc. vol. 94-12, 1994, p. 89.
[24] I. Yasuda, T. Hikita, J. Electrochem. Soc. 141 (1994) 1269.
[25] G.P. Khattak, D.E. Cox, Mat. Res. Bull. 12 (1977) 463.
[26] P.H. Larsen, P.V. Hendriksen, M. Mogensen, J. Therm. Anal. 49 (1997) 1263.
[27] P.V. Hendriksen, J.D. Carter, M. Mogensen, Proceedings of the Fourth International Symposium on SOFC, Yokohama, 18–23 June 1995, The Electrochemical Society, Proc. vol. 95-1, p. 934.
[28] I. Yasuda, M. Hishinuma, Proceedings of the Fourth International Symposium on SOFC, Yokohama, 18–23 June 1995, The Electrochemical Society, Proc. vol. 95-1, p. 924.
[29] P.V. Hendriksen, O. Jørgensen, Proceedings of the 17th Risø International Symposium on Material Science, High Temperature Electrochemistry: Ceramics and Metals, Risø National Laboratory, Denmark, 2–6 September 1996, p. 263.
[30] B. Sørensen, S. Sarraute, O. Jørgensen, A. Horsewell, Acta Mater. 46 (1998) 2603.

[31] J.W. Hutchinson, T.J. Lu, J. Eng. Mater. Technol. 117 (1995) 386.
[32] J.W. Stevenson, T.R. Armstrong, L.R. Pederson, W.J. Weber, in: H.U. Anderson, A.C. Khandkar, M. Liu (Eds.), Proceedings of the First International Symposium on Ceramic Membranes, 8–13 October 1995, The Electrochemical Society, Proc. vol. 95-24, p. 94.
[33] S. Pei, M.S. Kleefish, T.P. Kobylinski, J. Faber, C.A. Udovich, V. Zhang-McCoy, B. Dabrowski, U. Balachandran, R.L. Mieville, R.B. Poeppel, Catal. Lett. 30 (1995) 201.
[34] C. Tsai, A.G. Dixon, Y.H. Ma, W.R. Moser, M. Pascucci, J. Am. Ceram. Soc. 81 (1998) 1437.
[35] S. de Souza, S.J. Visco, L.C. De Jonghe, J. Electrochem. Soc. 144 (1997) L35.
[36] H. Anderson, C.C. Chen, L.W. Tai, M.M. Nasrallah, in: T.A. Ramanarayan, W.L. Worrel, H.L. Tuller (Eds.), Proceedings of the Second International Symposium on Ionic and Mixed Conducting Ceramics, The Electrochemical Society, Proc. vol. 94-12, 376.
[37] L.W. Tai, M.M. Nasrallah, H.U. Anderson, D.M. Sparlin, S.R. Sehlin, Solid State Ionics 76 (1995) 259–283.
[38] L.W. Tai, M.M. Nasrallah, H.U. Anderson, J. Solid State Chem. 118 (1995) 117.
[39] U. Balachandran, J.T. Dusek, S.M. Sweeney, R.B. Poebbel, R.L. Mieville, P.S. Mayia, M.S. Kleefish, S. Pei, T.P. Kobylinski, C.A. Udovich, A. Bose, Am. Ceram. Soc. Bull. 74 (1995) 71.